Modulation of COX-2 and NADPH oxidase-4 by Alpha-lipoic acid ameliorates busulfan-induced pulmonary injury in rats.

Mona Elhadidy (dr_monagaber@mans.edu.eg)
Mansoura University Faculty of Medicine https://orcid.org/0000-0002-8002-7478
Ahlam Elmasry
Mansoura University Faculty of Medicine
Hassan Reda Hassan Elsayed
Mansoura University Faculty of Medicine
Mohammad H El-Nablaway
Mansoura University Faculty of Medicine
Shereen Hamed
Mansoura University Faculty of Medicine
Mahmoud M. Elalfy
Mansoura University Faculty of Veterinary Medicine
Mohammed R. Rabei
Mansoura University Faculty of Medicine

Research Article

Keywords: Busulfan, Pulmonary fibrosis, α-lipoic acid (ALA), apoptosis, COX-2, NOX-4

Posted Date: March 18th, 2021

DOI: https://doi.org/10.21203/rs.3.rs-318983/v1

Version of Record: A version of this preprint was published at Heliyon on October 1st, 2021. See the published version at https://doi.org/10.1016/j.heliyon.2021.e08171.

Abstract

purpose: Busulfan is an antineoplastic drug that produces pulmonary fibrosis. This study aimed to explore the potential protective effect of α-lipoic acid on busulfan-induced pulmonary fibrosis in rats.

*Methods: Twenty-four a*dult male rats were divided into four groups: control, α-lipoic acid (ALA), busulfan, and busulfan plus α-lipoic acid. Lung index ratio, serum level of proinflammatory cytokine were assessed. The activities of antioxidant enzymes and lipid peroxidation products were estimated in the lung tissues in addition to histopathological analyses. The deposition of the collagen in the lung tissues was evaluated by Sirius red staining. The expressions of α-smooth muscle actin (α-SMA), TNF-α, and Caspase 3 were determined immunohistochemically. The pulmonary expression of COX-2 and NOX-4 mRNA were assessed using qRT-PCR.

Results: administration of ALA significantly ameliorated BUS-induced pulmonary fibrosis, besides the upregulation of antioxidants, and downregulation of pro-inflammatory cytokines. Also, it reduced collagen deposition associated with a decreased expression of α-SMA, TNF-α, and Caspase 3 in the lung tissues. Moreover, ALA significantly upregulated the expression of COX-2 concomitant with the downregulation of elevated NOX-4.

Conclusion: ALA attenuates the lung cytotoxicity of busulfan through its anti-inflammatory, anti-apoptotic, and antifibrotic effects that may be mediated by upregulation of COX-2 and downregulation of NOX-4.

Background

Pulmonary fibrosis is the commonest worldwide interstitial lung disease affecting more than five million individuals with an average survival time of about three years. Apart from inhaling mineral dust/asbestos and cigarette smoking, pulmonary fibrosis can be developed as an adverse toxic effect of anti-neoplastic drugs such as bleomycin and busulfan (Leger et al. 2017).

Busulfan (BUS) is an alkylating agent used for the treatment of neoplastic and autoimmune diseases (OLINER et al. 1961). As an alkylating agent, it works by sticking to one of the cancer cell's DNA strands and inhibits cell division (Iwamoto et al. 2004; Dun et al. 2012). Busulfan caused undesirable effects on the different body organs such as the liver, skin, bladder, nervous system, and gonads. Besides, it was associated with pulmonary toxicity that includes acute lung injury, chronic interstitial fibrosis, and alveolar hemorrhage (Iwamoto et al. 2004; Dun et al. 2012).

Alpha-lipoic acid (ALA, thioctic acid) is an organosulfur component present in plants, animals, and humans (Szeląg et al. 2012; Moura et al. 2015). Naturally, ALA is located in the mitochondria, where it acts as a cofactor for some enzymatic complexes involved in the Krebs cycle. Also, ALA acts as an antioxidant and also able to increases and repairs the intrinsic antioxidant systems and supports their production (Han et al. 1997; Shay et al. 2009; Gorąca et al. 2011).

This study aims to examine the potential effect of ALA on a rat model of pulmonary fibrosis induced by intraperitoneal (i.p.) administration of busulfan and to evaluate its antioxidant, anti-inflammatory, anti-apoptotic and antifibrotic effects. Moreover, the possible intracellular pathway of ALA was also examined concerning COX-2 activation and NOX-4 suppression.

Methods

Experimental design:

A total of 24 adult albino male rats (200-240 g weight) were obtained from Medical Experimental Research Center (MERC), Mansoura Faculty of Medicine, Egypt. Rats were acclimatized for one week before initiation of the experiment, where the room temperature was controlled at 24 ± 5 and 45 to 55% humidity with a regular 12:12 h light-dark cycle. All animals were given water and food ad libitum. The protocol of this experimental study followed the Guide for the Care and Use of Laboratory Animals (Institute for Laboratory Animal Research, National Research Council, Washington, DC and National Academy Press, no. 85-23, revised 1996). Our Local Committee of Animal Care and Used approved this protocol (Code number: R.20.08.993).

After acclimatization, the rats randomly divided into 4 groups, each contains 6 rats: the normal control group, received phosphate buffer solution (PBS), ALA group, normal rats intraperitoneally injected once daily with α-lipoic acid (20 mg/kg/day for 6 weeks) (Liu et al. 2007), BUS induced lung injury group, the rats were received two doses of BUS by (i.p.) injection with 14 days interval. Each dose was 15 mg/kg dissolved in 0.5 mL PBS (Aboul Fotouh et al. 2018), BUS+ ALA group, α-lipoic acid was given on top of busulfan in the same previous doses (20 mg/kg/day for 6 weeks). Both BUS and ALA were purchased from Sigma Aldrich Chemical Co. (St. Louis, MO, USA).

After six weeks from the beginning of the experiment, all rats were weighed then deeply anesthetized with thiopental sodium. Blood samples were collected directly from the heart, for subsequent biochemical analysis. Animals were weighted then the lung was removed and weighed to determine the lung index which was determined by dividing lung weight (g) by body weight (g) and multiplying by 100. One of the lung lobes was preserved in formaldehyde solution for histopathological and immunohistochemical examinations. The other one was weighed and divided into two halves, one half was stored at −20 °C for detection of enzyme activities and level of PGE2 while the other half was preserved in RNAlater Stabilization Solution (ThermoFisher Scientific) at 4°C overnight before being stored at −80°C until isolation of total RNA and subsequent real-time RT-PCR.

Measurement of TNF-α, IL-1β, IL-6, and IL-10 serum levels:

Serum levels of TNF-α, IL-1β, IL-6, and IL-10 cytokines were determined using an enzyme-linked immunosorbent assay kit (Bioscience Co., USA) according to the manufacturer's instructions. The absorbance was read at 450nm using a plate reader.

Activities of enzymatic antioxidants:

Superoxide dismutase (SOD) activity was assessed in homogenized lung tissues by a commercially available standard enzymatic kit (Cayman Chemical Company, USA). The absorbance was read at 440–460 nm. Glutathione peroxidase (GPx) activity was measured in lung tissues by using a commercially available kit (Cayman Chemical, USA) and the absorbance was read once every minute at 340 nm.

Estimation of lipid peroxidation product:

Lipid peroxidation was determined in the form of malondialdehyde (MDA) by the method of Ohkawa et al. (Ohkawa et al. 1979). MDA was assessed in the rats' lung tissues with ELISA kits (R&D system), according to the manufacturer's protocols. The absorbance was measured at 532 nm.

Measurement of PGE2 levels in lung tissues:

The levels of PGE2 were measured in the lung tissues by a competitive enzyme immunoassay kit (Abcam, ab133021, Cambridge, UK) following the manufacturer's protocol. The absorbance of PEG2 was measured at 405 nm with a microplate reader.

Measurement of hydroxyproline in the lung tissues:

Hydroxyproline content of the lung tissue assay was performed using a commercially available ELISA kit (Hangzhou Eastbiopharm Co., Ltd., China). The absorbance was read at 450nm using a plate reader.

Histopathological techniques:

Lung was dissected and fixed in 10% (neutral) formalin, cleansed through running water, dehydrated gradually by increasing concentrations of alcohol, cleared by xylene, and then embedded in paraffin blocks. Sections were cut at 3-5 um. and stained with hematoxylin-eosin (H&E) as described by Bancroft and Christopher (Bancroft, J.D.; Christopher 2019). Lung sections were examined microscopically and photomicrographed.

Immunohistochemical staining:

Immunohistochemistry was done on 3-4µm thick sections which were mounted on charged slides and then analysis was done through the immunoperoxidase method. Concisely, deparaffinization of the sections was performed, then they were treated with H_2O_2 (0.3 %)/methanol for 10 minutes at room temperature to block endogenous peroxidase activity. Antigen retrieval was achieved by heating sections in 10 mM citrate buffer for 10 min at 95-100C (PH 6) then allowed to cool at room temperature for 1 hour. Sections were left with the primary antibodies for Caspase3 as a marker for apoptotic activity, TNF-α as a marker for inflammation and macrophage activity, and Alpha smooth muscle actin (α-SMA) as a fibrogenic marker (Servicebio; Cat. No. GB11532 (rabbit polyclonal antibody), Santa Cruz; sc-52746 (mouse monoclonal antibody) and Thermoscientific; MS-113-RQ (mouse monoclonal antibody),

respectively) overnight at 4ºC (1:800, 1:50 and 1:800 dilutions, respectively). Then, sections were incubated in Diaminobenzidine (DAB) reagent to demonstrate peroxidase activity. The sections were left in PBS at 4ºC overnight. Incubation of the slides with universal mouse/rabbit polydetector plus (BSB 0257, Bio SB) for half an hour was done then washed by PBS to identify the primary antibody binding. Finally, DAB was added for 4 min then the sections were counterstained with hematoxylin. For the negative control, we replaced the primary antibody with PBS. The sections were then washed, dehydrated, and examined by a light microscope. Dark brown areas in the cytoplasm or nucleus demonstrate positive staining and the background is blue (Ramos-Vara and Miller 2014).

Quantification of mRNA by real-time reverse transcription-PCR (qRT-PCR):

Lung tissue samples were preserved in RNA later (500 ul were used for each 50 mg tissue sample) (Qiagen, Germany), incubated overnight at 2–8°C then removed from the reagent and transferred to -80°C for storage until processing. On the processing, lung tissue samples were homogenized by five strokes of liquid nitrogen. Total cellular RNA was extracted using the QIAzol reagent (Qiagen, Germany), according to the manufacturer's specifications. The RNA yield was checked by Thermo Scientific NanoDrop 2000 (USA) for the concentration using the absorbance at 260 nm, and for the purity using 260/280 and 260/230 ratios. Reverse transcription of 1ug of RNA was done using SensiFAST™ cDNA Synthesis Kit (Bioline, UK) using the following program (10 minutes at 25°C for primer annealing, 15 minutes at 42°C for reverse transcription, and 85°C for 5 minutes for inactivation) on Applied Biosystems 2720 Thermal Cycler. cDNA templates were amplified using a real-time PCR instrument (Pikoreal 96, ThermoScientific). The amplification reaction contained a 20 μl total volume mixture [10 μl of HERA SYBR green PCR Master Mix (Willowfort, UK), 2 μl of cDNA template, 2 µl (10 pmol) gene primer and 6 μl of nuclease-free water], and by using the following program: 95°C for 2 min, 40 cycles of 95°C for 10 s, 60°C for 30 s. The sequences of the used primer pairs are supplied in **Table (1)**, Glyceraldehyde-3-phosphate dehydrogenase (GAPDH) was used as a housekeeping gene. The primer sets were checked for specificity using the Primer-BLAST program **[http**s://www.ncbi.nlm.nih.gov/tools/primer-blast/]. The specificity of the PCR products was also evaluated by the melting curve analysis. Primer sets were synthesized by Vivantis (Vivantis Technologies, Malaysia). Relative gene expression levels were represented as $^{\Delta}$Ct = Ct target gene– Ct housekeeping gene; fold change of gene expression was calculated according to the $2^{-\Delta\Delta CT}$ method (Livak and Schmittgen 2001). PCR products were run on 3% agarose gels and visualized on a UV transilluminator (OWI Scientific, France). Then, the gels were photographed using Bio-Rad gel

Table (1): The sequence of rat primers used in the qRT-PCR analysis:

Gene	Sequence	Product size
Cyclo-oxygenase 2 (COX-2)	**Forward primer**: GGAGCAACCGATGTGGAATTG **Reverse primer**: GCCGGTATCTGCCTTCATGT	104 bp
NADPH oxidase 4 (NOX-4)	**Forward primer**: TGTTGGGCCTAGGATTGTGT **Reverse primer**: CTTCTGTGATCCGCGAAGGT	119 bp
Glyceraldehyde-3-phosphate dehydrogenase (GAPDH)	**Forward primer**: TGCCACTCAGAAGACTGTGG **Reverse primer**: GGATGCAGGGATGATGTTCT	85 bp

Statistical analysis:

Data were analyzed using the **SPSS program** (version 21). First, the normality of data was tested using the Shapiro test. Descriptive data (means ± SDM) were calculated for each dependent variable. Overall, group differences analyzed using a one-way ANOVA followed by post-hoc Tuckey's HSD test. $P \leq 0.05$ was used as the decision rule for significance testing.

Results

Effect of ALA on the body weight and lung indicesin BUS-induced lung fibrosis rat model:

BUS administration induces a significantly lower body weight associated with a significantly higher lung index in comparison to those of normal ones ($p < 0.01$, $p < 0.01$, respectively). However, the lower body weight in the BUS group was significantly increased by the administration of ALA treatment ($P< 0.01$). Also, both normal and fibrotic rats who received ALA exhibited a significantly higher body weight when compared to that of other groups ($P< 0.01$), figure (1).

Effects of ALA on the inflammatory markers in BUS-induced lung fibrosis rat model:

BUS induced a significantly higher serum levels of TNF-α ($p < 0.001$), IL-1β ($p < 0.01$), IL-6 ($p< 0.001$) and IL-10 ($p < 0.001$) in comparison to those of the normal rats. However, ALA treatment significantly mitigated the elevated levels of TNF-α ($p < 0.001$), IL-1β ($p < 0.01$), IL-6 level ($p<0.001$) and IL-10 level ($p <$

0.001) in comparison to those of BUS group. Moreover, normal rats who received ALA exhibited a lower level of these cytokines relative to those of control one, figure (2).

Effects of ALA on the antioxidant enzymes and oxidative stress markers in the lung tissues of BUS-induced lung fibrosis rat model:

A significantly higher MDA level was noticed in the lung tissues of the BUS group compared to those of the normal group ($p< 0.001$). Moreover, significantly lower activities of GPx and SOD enzyme were observed in BUS-induced lung fibrotic rats in comparison to those of the control ones ($p < 0.01$). On contrary, treatment of the fibrotic rats with ALA produced a significantly higher level of MDA ($p < 0.001$) and restored both GPx and SOD enzyme activities ($p < 0.01$) in comparison to those of the BUS group, **figure (3)**.

Effect of ALA on the level of PGE2 in BUS-induced lung fibrosis:

BUS induced a significantly higher level of PGE2 in the lung tissues relative to that of normal ones ($p < 0.001$). However, the treatment of the fibrotic rats with ALA exhibited a significant elevation in the level of PGE2 compared to the BUS group ($p < 0.001$), **figure (4)**.

Effect of ALA on hydroxyproline and collagen deposition in the lung tissue of BUS-induced lung fibrosis rat model:

Administration of BUS induced significantly more hydroxyproline content in the lung tissues relative to its level in the normal group ($p < 0.05$). On the other hand, the treatment of the fibrotic rats with ALA produced significantly less hydroxyproline in ALA treated rats relative to the untreated BUS group ($p < 0.05$). Moreover, supplementation of normal rats with ALA induced a significant decrease in the hydroxyproline content relative to the control group ($P< 0.004$), **figure (5)**.

Histopathological evaluation:

In H&E-stained sections, the lung of the rats received normal saline or ALA alone revealed normally organized architecture with thin interalveolar septa **Figure (6A, B).** While, the lung tissues of the untreated BUS group revealed the disorganization of lung architecture, cellular infiltration in the interalveolar septa associated with the presence of intraluminal cellular debris in pulmonary bronchiole, **Figure (6C).** Rats treated with ALA showed almost normal architecture of pulmonary tissues associated with an obvious reduction in cellular infiltration, **Figure (6D)**. The percentage area stained with Sirius red in the BUS group showed a significant increase ($p < 0.05$) compared to the control group, **Figure (7C)**. On the other hand, the percentage area stained with Sirius red in the BUS+ALA group was markedly reduced relative to the untreated BUS group ($p < 0.05$) **Figure (7D)**.

Effect of ALA on the immunohistochemical expression of α-SMA in BUS-induced lung fibrosis:

A significantly higher expression of α-SMA was noted in the untreated BUS rats' lungs in comparison to that of the normal rats ($p < 0.001$). On the other hand, the fibrotic rats who received ALA showed a lower expression of α-SMA in comparison to that of the non-treated BUS rats ($p < 0.001$). Supplementation of normal rats with ALA exhibited a lower expression of α-SMA immunoreactive cells relative to that of the control group. **Figure (8)**

Effect of ALA on the immunohistochemical expression of TNF-α in BUS-induced lung fibrosis:

A significantly higher expression of TNF-α was recorded in the untreated BUS rats' lungs in comparison to that of the normal rats ($p < 0.01$). Meanwhile, the fibrotic rats who received ALA showed a markedly lower expression of TNF-α in comparison to that of the non-treated BUS rats ($p < 0.01$). Moreover, the administration of ALA to the normal non-fibrotic rats showed a markedly lower expression of TNF-α relative to that of the control result. **Figure (9)**

Effect of ALA on the immunohistochemical expression of Caspase-3 in BUS-induced lung fibrosis:

The results revealed significantly more Caspase-3 immunoreactive cells in the BUS group than that of the normal ones ($p < 0.05$). In contrast, relative to the BUS group, the ALA-treated fibrotic groups showed a lower number of Caspase-3 immunoreactive cells ($p < 0.05$). While ALA in normal non-fibrotic rats did not show any significant change in Caspase-3 expression relative to that of the control ones, **Figure (10).**

Effect of ALA on the expression of COX-2 in BUS-induced lung fibrosis:

The results showed significantly less COX-2 expression at the mRNA level in the non-treated BUS group relative to that of the control ones ($p < 0.004$). In contrast, when the comparison was made to the BUS group, the ALA-treated fibrotic groups showed markedly more COX-2 expression ($p < 0.05$). While ALA in normal non-fibrotic rats didn't show any significant change in COX-2 expression as compared to that of the control one. **Figure (11)**

Effect of ALA on the expression of NOX-4 in BUS-induced lung fibrosis:

The results presented in **Figure (12)** showed a significantly higher expression of NOX-4 mRNA in the untreated BUS rats' lungs relative to the normal results ($p < 0.001$). On the other hand, the fibrotic rats who received ALA supplementation showed markedly lower expression of NOX-4 mRNA relative to that of the non-treated BUS rats ($p< 0.001$). Furthermore, the administration of ALA to the normal non-fibrotic rats showed non-significant changes in the expression of this gene relative to that of the control result.

Discussion

In the current work, we investigated the potential protective effect of ALA against pulmonary injury induced by BUS in rats. Our data revealed a significant decrease in the rats' body weights with a marked increase in the lung index in the BUS group. The increase in the weight of the lung indicates the occurrence of pulmonary fibrosis which may be explained by transferring the alkyl group(s) which present

in BUS to different body cells to induce lung injury in the form of fibrosis (Ahar et al. 2014). On the other hand, the administration of ALA to the fibrotic rats exhibited a significant elevation in the bodyweight with a marked decline in the lung index. These findings indicating that the ALA administration conferred significant protection against BUS-induced lung injury.

The obtained data from the serum analysis revealed a significant elevation in the levels of TNF-α and IL-1β and IL-6 in the BUS group. Chitra et al., 2013 reported that increased proinflammatory cytokines during the inflammatory response could be responsible for the formation of the fibroblasts and the release of profibrogenic cytokine (TGF-β) and subsequent deposition of collagen. On contrary, the administration of ALA significantly reduced the elevated levels of these proinflammatory cytokines in BUS administrated rats. These results indicate the beneficial effect of ALA against BUS-induced lung fibrosis that may be mediated by the reduction of proinflammatory cytokine production. ALA treatment attenuates the upregulation of cytokines and displays powerful anti-inflammatory effects.

IL-10 levels have been reported to be markedly increased in multiple experimental models of pulmonary inflammation and fibrosis (Park et al. 2011; Kim et al. 2016). Consistent with these previous studies, our results revealed a significant elevation in the serum level of IL-10 of BUS administered rats. Doughty et al., 1998 explained this increase in the level of IL-10 to be a compensatory anti-inflammatory response and to be proportionate with the already released pro-inflammatory cytokines. On the other hand, the ALA administration significantly reduced the serum level of IL-10. The down-regulation of IL-10 may be an additional pathway involved in its beneficial anti-inflammatory effects. It is associated with a decrease in the level of pro-inflammatory cytokines.

Daniil et al. (Daniil et al. 2008) demonstrated that oxidative stress plays a chief role in pulmonary fibrosis. The generation of reactive oxygen species (ROS) and reactive nitrogen species has been reported to be implicated in the pathogenesis of fibrosis (Fubini and Hubbard 2003; Bargagli et al. 2009). Moreover, the markers of oxidative stress have been identified in the patients' lung suffering from pulmonary fibrosis and also in animal models of lung fibrosis (Chitra et al. 2013). In the present study, the administration of BUS significantly compromised oxidants/antioxidants hemostasis as manifested by a significant elevation of MDA content in the lung tissues concomitant with a reduction in the activities of GPx and SOD. Meanwhile, treatment of fibrotic rats with ALA restores the cellular redox activity, these results indicate the ability of ALA to maintain oxidant-antioxidant balance.

In context to all aforementioned alterations, the histopathological changes manifested by disorganization of the lung architecture increased cellular infiltration, and the presence of intraluminal cellular debris in the pulmonary bronchiole was observed following BUS administration. These findings were following the study of Ida et al. (Ida et al. 2016). These histological alterations were markedly corrected upon the ALA administration. Overall, our results indicate that ALA could be beneficial against BUS-induced lung fibrosis. This was supported by the finding conducted by Azmoonfar et.al. (Azmoonfar et al. 2019) who reported that ALA was able to mitigate fibrosis and pneumonitis markers in mice lung tissues following lung irradiation.

Excessive collagen deposition is a vital phenomenon in pulmonary fibrosis. As previously known, anti-neoplastic drugs such as busulfan induce the production of free radicals, upregulating the synthesis of collagen in the lungs. Furthermore, the administration of BUS encourages cytokine dysregulation and the development of inflammation that activate the fibroblasts leading to an imbalance between collagen deposition and reabsorption (Kinnula and Myllärniemi 2008). In agreement with these previous data, the present study, revealed an obvious increase in the hydroxyproline content in the BUS group while it was decreased markedly in the fibrotic rats treated with ALA. Both normal groups (control and ALA) show normal collagen distribution in both pulmonary interstitium and bronchiolar wall, whereas in the BUS group the lung section shows excessive collagen deposition in the pulmonary interstitium and surrounding alveolar wall. On the other hand, the lung section of fibrotic rats treated with ALA revealed less marked interstitial collagen deposition. This effect of ALA could be explained by possible mechanisms such as inhibiting lung inflammatory cell accumulation and thus reducing ROS production, removal of the free radicals from the lung tissues, detoxifying free radicals generated by BUS, and eventually inhibition of fibroblast activation and proliferation.

The mechanisms of pulmonary fibrosis are still unclear. Several researchers found that apoptosis may contribute to the deposition of collagen and the progression of pulmonary fibrosis through modulation of immune response and paracrine signaling (Wang et al. 2000, 2006; Barbas-Filho et al. 2001). The previous study showed that direct administration of apoptotic cells to the rats' lungs induced pulmonary inflammation and fibrosis indicating a direct relationship between apoptosis and the detected lung pathologies (Wang et al. 2006). In agreement with these previous studies, our results demonstrated that the expression of apoptotic cells, Capase3 immunoreactive cells, in the lung of the BUS group was significantly higher than the control ones and this finding indicating the involvement of Caspase-dependent apoptotic signaling pathways in the BUS-induced lung injury. On the other hand, we noticed a significant decrease in the expression of Caspase-3 immunoreactive cells in ALA-treated rats which may suggest its powerful anti-apoptotic effect.

Furthermore, our findings illustrate a remarkable increase in the number of α-SMA -positive cells in the areas of active fibrosis, which become prominent with increased collagen deposition in the BUS group. TGF-β1 is considered the most powerful profibrogenic cytokine (Bancroft, J.D.; Christopher 2019). TGF-β1 can encourage the secretion of collagens from the pulmonary fibroblasts and/or induce transformation of fibroblasts to myofibroblasts that express α-SMA; both are critical steps in the initiation and progression of pulmonary fibrosis (Horowitz et al. 2007; Tseng et al. 2013). And this could be explained in our results, as there was a remarkable increase in the serum level of pro-inflammatory cytokines that responsible for the formation of the fibroblasts and the release of TGF-β. Meanwhile, fibrotic rats treated with ALA exhibited a marked decrease in the number of α-SMA -immunoreactive cells associated with a decline in collagen deposition and hydroxyproline content in the lung tissue. It was concomitant with a significant decrease in the serum level of pro-inflammatory cytokines. All these results indicating the anti-fibrotic effect of ALA against BUS-induced pulmonary fibrosis which may be related to its anti-inflammatory, antioxidant, and anti-apoptotic effects.

Many pieces of evidence suggest that PGE2 may play a role in limiting fibrotic responses in the lung and this pathway may be attenuated in patients with pulmonary fibrosis. Previous reports observed that patients with idiopathic pulmonary fibrosis exhibited a marked decrease in the expression of COX-2 and subsequently reduced PGE2 production in bronchoalveolar fluid and fibroblasts (Wilborn et al. 1995; Vancheri et al. 2000; Bozyk and Moore 2011). Moreover, Maher et al. (Maher et al. 2010) demonstrated a decline in the expression of both COX-2 and PGE2 in the fibroblasts from patients suffering from pulmonary fibrosis. they suggested that these low levels of COX-2 and PGE2 promote survival of fibroblast and prevent its apoptosis in the fibrotic lung. Moreover, Ex-vivo studies have shown that PGE2 can decrease proliferation, activation, and collagen synthesis from pulmonary fibroblasts (McAnulty et al. 1997; Kohyama et al. 2001; Kolodsick et al. 2003; Lovgren et al. 2006; Huang et al. 2010). Besides, several early studies using mice lacking COX-2 suggested that COX-2-derived prostaglandins could limit some aspects of the histological changes and collagen production in the bleomycin and vanadium pentoxide models of lung fibrosis (Keerthisingam et al. 2001; Bonner et al. 2002). A decreased expression of COX-2 which was associated with a marked decrease in the level of PGE2 in the non-treated BUS group was observed in this study. T + he administration of ALA significantly increased COX-2 mRNA levels in the fibrotic lung and subsequently increased the level of PGE2 in the lung tissue. These results proposed that the protective effects of ALA against BUS-induced lung damage may be mediated by restoring the normal level of COX-2 and PGE2.

Among seven isoforms of NADPH oxidases (NOXes), NOX-4 has been found to modulates the TGF-β/SMAD-signaling through intracellular production of ROS (Jiang et al. 2014). It has been recently shown that NOX-4 is expressed in the pulmonary arterial adventitial fibroblasts and contributes to the ROS generation under hypoxic conditions. It subsequently stimulates proliferation, activation, and inhibiting apoptosis of fibroblasts (Hecker et al. 2009). Furthermore, NOX-4 is involved in the differentiation of human cardiac fibroblasts into myofibroblasts through TGF-β1 (Amara et al. 2010). In agreement with these previous findings, the current work demonstrated a marked elevation in the expression of NOX-4 mRNA in the BUS rats' lung tissue. However, the administration of ALA mitigates this increase in the levels of NOX-4 which is associated with attenuating lung fibrosis and decreases the expression of α-SMA. This finding is suggesting that the anti-fibrotic effect of ALA is mainly mediated through inhibition of myofibroblast differentiation. Accordingly, we proposed that the regulation of NOX-4 expression by ALA can be a promising anti-fibrotic modality for fibrotic lung disorders induced by BUS therapy. This conclusion is supported by decrease collagen deposition in lung tissue (hydroxyproline and Sirius red stain) with the decline in the number of α-SMA immunoreactive cells in the BUS group treated with ALA.

Conclusions

According to our results, ALA may be considered as a potential inhibitor of BUS-induced pulmonary fibrosis through its antioxidant, anti-inflammatory, antiapoptotic and antifibrotic effects as determined by biochemical and semiquantitative morphological indices of lung injury. Also, it exerts a powerful improvement in the deposition of collagen via the upregulation of COX-2 expression in lung tissue with an increase in the level of PGE2 and downregulation of NOX-4 mRNA expression. Thus, ALA may have

promise in the prevention of BUS-induced lung damage. However, further studies are needed to explore the mechanism of the valuable effect of ALA in the management of pulmonary fibrosis.

Declarations

- **Funding:** No funding was received for conducting this study.
- **Competing interests**: The authors declare that they have no competing interests
- **Availability of data and material** (data transparency); Available
- **Code availability** (software application or custom code): not applicable
- **Authors' contributions**: The authors declare that all data were generated in-house and that no paper mill was used. All authors contributed to the study conception and design. Material preparation, data collection, and analysis were performed by Mona G. Elhadidy, Mohammed R. Rabei, Ahlam Elmasry and Mahmoud M. Elalfy. The first draft of the manuscript was written by Mona G. Elhadidy. Biochemical analysis and PCR were done by Mohammad H El-Nablaway. Histopathological and immunohistochemical evalution were done by Hassan Reda Hassan Elsayed and Shereen Hamed. Reviewing and editing were done by Mona G. Elhadidy and Ahlam Elmasry. All authors read and approved the final manuscript.
- **Ethics approval**: The protocol of this experimental study followed the Guide for the Care and Use of Laboratory Animals (Institute for Laboratory Animal Research, National Research Council, Washington, DC and National Academy Press, no. 85-23, revised 1996). Our Local Committee of Animal Care and Used approved this protocol (Code number: R.20.08.993).
- **Consent to participate**: Not applicable.
- **Consent for publication**: not applicable

References

Aboul Fotouh GI, Abdel-Dayem MM, Ismail DI, Mohamed HH (2018) Histological Study on the Protective Effect of Endogenous Stem Cell Mobilization in Busulfan-Induced Testicular Injury in Albino Rats. J Microsc Ultrastruct 6:197–204. https://doi.org/10.4103/JMAU.JMAU_35_18

Ahar NH, Khaki A, Akbari G, Novin MG (2014) The effect of Busulfan on body weight, Testis weight and MDA enzymes in male rats. Int J Women's Heal Reprod Sci 2:316–319. https://doi.org/10.15296/ijwhr.2014.52

Amara N, Goven D, Prost F, et al (2010) NOX4/NADPH oxidase expression is increased in pulmonary fibroblasts from patients with idiopathic pulmonary fibrosis and mediates TGFbeta1-induced fibroblast differentiation into myofibroblasts. Thorax 65:733–738. https://doi.org/10.1136/thx.2009.113456

Azmoonfar R, Amini P, Yahyapour R, et al (2019) Mitigation of Radiation-induced Pneumonitis and Lung Fibrosis using Alpha-lipoic Acid and Resveratrol. Antiinflamm Antiallergy Agents Med Chem 19:149–157.

https://doi.org/10.2174/1871523018666190319144020

Bancroft, J.D.; Christopher L (2019) . (2019) The hematoxylins and eosin. And connective and other mesenchymal tissues with their stains In: Kim S Suvarna, Christopher Layton, John D. Bancroft(Eds.), Bancroft'S Theory and Practice of Histological Techniques 8th. In: Kim S Suvarna, Christopher Layton, John D. Bancroft(Eds.), Bancroft'S Theory and Practice of Histological Techniques 8thChurchill Livingstone Elsevier, Oxford,. England, pp 126–138&153–175

Barbas-Filho J V, Ferreira MA, Sesso A, et al (2001) Evidence of type II pneumocyte apoptosis in the pathogenesis of idiopathic pulmonary fibrosis (IFP)/usual interstitial pneumonia (UIP). J Clin Pathol 54:132–138. https://doi.org/10.1136/jcp.54.2.132

Bargagli E, Olivieri C, Bennett D, et al (2009) Oxidative stress in the pathogenesis of diffuse lung diseases: a review. Respir Med 103:1245–1256. https://doi.org/10.1016/j.rmed.2009.04.014

Bonner JC, Rice AB, Ingram JL, et al (2002) Susceptibility of cyclooxygenase-2-deficient mice to pulmonary fibrogenesis. Am J Pathol 161:459–470. https://doi.org/10.1016/S0002-9440(10)64202-2

Bozyk PD, Moore BB (2011) Prostaglandin E2 and the pathogenesis of pulmonary fibrosis. Am J Respir Cell Mol Biol 45:445–452. https://doi.org/10.1165/rcmb.2011-0025RT

Chitra P, Saiprasad G, Manikandan R, Sudhandiran G (2013) Berberine attenuates bleomycin induced pulmonary toxicity and fibrosis via suppressing NF-κB dependant TGF-β activation: a biphasic experimental study. Toxicol Lett 219:178–193. https://doi.org/10.1016/j.toxlet.2013.03.009

Daniil ZD, Papageorgiou E, Koutsokera A, et al (2008) Serum levels of oxidative stress as a marker of disease severity in idiopathic pulmonary fibrosis. Pulm Pharmacol Ther 21:26–31. https://doi.org/10.1016/j.pupt.2006.10.005

Doughty L, Carcillo JA, Kaplan S, Janosky J (1998) The compensatory anti-inflammatory cytokine interleukin 10 response in pediatric sepsis-induced multiple organ failure. Chest 113:1625–1631. https://doi.org/10.1378/chest.113.6.1625

Dun MD, Aitken RJ, Nixon B (2012) The role of molecular chaperones in spermatogenesis and the post-testicular maturation of mammalian spermatozoa. Hum Reprod Update 18:420–435. https://doi.org/10.1093/humupd/dms009

Fubini B, Hubbard A (2003) Reactive oxygen species (ROS) and reactive nitrogen species (RNS) generation by silica in inflammation and fibrosis. Free Radic Biol Med 34:1507–1516. https://doi.org/10.1016/s0891-5849(03)00149-7

Gorąca A, Huk-Kolega H, Piechota A, et al (2011) Lipoic acid - biological activity and therapeutic potential. Pharmacol Rep 63:849–858. https://doi.org/10.1016/s1734-1140(11)70600-4

Han D, Handelman G, Marcocci L, et al (1997) Lipoic acid increases de novo synthesis of cellular glutathione by improving cystine utilization. Biofactors 6:321–338. https://doi.org/10.1002/biof.5520060303

Hecker L, Vittal R, Jones T, et al (2009) NADPH oxidase-4 mediates myofibroblast activation and fibrogenic responses to lung injury. Nat Med 15:1077–1081. https://doi.org/10.1038/nm.2005

Horowitz JC, Rogers DS, Sharma V, et al (2007) Combinatorial activation of FAK and AKT by transforming growth factor-beta1 confers an anoikis-resistant phenotype to myofibroblasts. Cell Signal 19:761–771. https://doi.org/10.1016/j.cellsig.2006.10.001

Huang SK, Fisher AS, Scruggs AM, et al (2010) Hypermethylation of PTGER2 confers prostaglandin E2 resistance in fibrotic fibroblasts from humans and mice. Am J Pathol 177:2245–2255. https://doi.org/10.2353/ajpath.2010.100446

Ida T, Hashimoto S, Suzuki N, et al (2016) [Multiple organ failure presumably due to alkylating agents used as preconditioning drugs for autologous peripheral blood stem cell transplantation in an acute promyelocytic leukemia]. Rinsho Ketsueki 57:41–46. https://doi.org/10.11406/rinketsu.57.41

Iwamoto T, Hiraku Y, Oikawa S, et al (2004) DNA intrastrand cross-link at the 5'-GA-3' sequence formed by busulfan and its role in the cytotoxic effect. Cancer Sci 95:454–458. https://doi.org/10.1111/j.1349-7006.2004.tb03231.x

Jiang F, Liu G-S, Dusting GJ, Chan EC (2014) NADPH oxidase-dependent redox signaling in TGF-β-mediated fibrotic responses. Redox Biol 2:267–272. https://doi.org/10.1016/j.redox.2014.01.012

Keerthisingam CB, Jenkins RG, Harrison NK, et al (2001) Cyclooxygenase-2 deficiency results in a loss of the anti-proliferative response to transforming growth factor-beta in human fibrotic lung fibroblasts and promotes bleomycin-induced pulmonary fibrosis in mice. Am J Pathol 158:1411–1422. https://doi.org/10.1016/s0002-9440(10)64092-8

Kim BG, Lee PH, Lee SH, et al (2016) Long-Term Effects of Diesel Exhaust Particles on Airway Inflammation and Remodeling in a Mouse Model. Allergy Asthma Immunol Res 8:246–256. https://doi.org/10.4168/aair.2016.8.3.246

Kinnula VL, Myllärniemi M (2008) Oxidant-antioxidant imbalance as a potential contributor to the progression of human pulmonary fibrosis. Antioxid Redox Signal 10:727–738. https://doi.org/10.1089/ars.2007.1942

Kohyama T, Ertl RF, Valenti V, et al (2001) Prostaglandin E(2) inhibits fibroblast chemotaxis. Am J Physiol Lung Cell Mol Physiol 281:L1257-63. https://doi.org/10.1152/ajplung.2001.281.5.L1257

Kolodsick JE, Peters-Golden M, Larios J, et al (2003) Prostaglandin E2 inhibits fibroblast to myofibroblast transition via E. prostanoid receptor 2 signaling and cyclic adenosine monophosphate elevation. Am J

Respir Cell Mol Biol 29:537–544. https://doi.org/10.1165/rcmb.2002-0243OC

Leger P, Limper AH, Maldonado F (2017) Pulmonary Toxicities from Conventional Chemotherapy. Clin Chest Med 38:209–222. https://doi.org/10.1016/j.ccm.2017.01.002

Liu R, Ahmed KM, Nantajit D, et al (2007) Therapeutic effects of α-lipoic acid on bleomycin-induced pulmonary fibrosis in rats. Int J Mol Med 19:865–873. https://doi.org/10.3892/ijmm.19.6.865

Livak KJ, Schmittgen TD (2001) Analysis of relative gene expression data using real-time quantitative PCR and the 2(-Delta Delta C(T)) Method. Methods 25:402–408. https://doi.org/10.1006/meth.2001.1262

Lovgren AK, Jania LA, Hartney JM, et al (2006) COX-2-derived prostacyclin protects against bleomycin-induced pulmonary fibrosis. Am J Physiol Lung Cell Mol Physiol 291:L144-56. https://doi.org/10.1152/ajplung.00492.2005

Maher TM, Evans IC, Bottoms SE, et al (2010) Diminished prostaglandin E2 contributes to the apoptosis paradox in idiopathic pulmonary fibrosis. Am J Respir Crit Care Med 182:73–82. https://doi.org/10.1164/rccm.200905-0674OC

McAnulty RJ, Hernández-Rodriguez NA, Mutsaers SE, et al (1997) Indomethacin suppresses the anti-proliferative effects of transforming growth factor-beta isoforms on fibroblast cell cultures. Biochem J 321 (Pt 3:639–643. https://doi.org/10.1042/bj3210639

Moura FA, de Andrade KQ, dos Santos JCF, Goulart MOF (2015) Lipoic Acid: its antioxidant and anti-inflammatory role and clinical applications. Curr Top Med Chem 15:458–483. https://doi.org/10.2174/1568026615666150114161358

Ohkawa H, Ohishi N, Yagi K (1979) Assay for lipid peroxides in animal tissues by thiobarbituric acid reaction. Anal Biochem 95:351–358. https://doi.org/10.1016/0003-2697(79)90738-3

OLINER H, SCHWARTZ R, RUBIO F, DAMESHEK W (1961) Interstitial pulmonary fibrosis following busulfan therapy. Am J Med 31:134–139. https://doi.org/10.1016/0002-9343(61)90229-7

Park E-J, Roh J, Kim S-N, et al (2011) A single intratracheal instillation of single-walled carbon nanotubes induced early lung fibrosis and subchronic tissue damage in mice. Arch Toxicol 85:1121–1131. https://doi.org/10.1007/s00204-011-0655-8

Ramos-Vara JA, Miller MA (2014) When tissue antigens and antibodies get along: revisiting the technical aspects of immunohistochemistry--the red, brown, and blue technique. Vet Pathol 51:42–87. https://doi.org/10.1177/0300985813505879

Shay KP, Moreau RF, Smith EJ, et al (2009) Alpha-lipoic acid as a dietary supplement: molecular mechanisms and therapeutic potential. Biochim Biophys Acta 1790:1149–1160.

https://doi.org/10.1016/j.bbagen.2009.07.026

Szeląg M, Mikulski D, Molski M (2012) Quantum-chemical investigation of the structure and the antioxidant properties of α-lipoic acid and its metabolites. J Mol Model 18:2907–2916. https://doi.org/10.1007/s00894-011-1306-y

Tseng CM, Hsiao YH, Su VYF, et al (2013) The suppression effects of thalidomide on human lung fibroblasts: Cell proliferation, vascular endothelial growth factor release, and collagen production. Lung 191:361–368. https://doi.org/10.1007/s00408-013-9477-1

Vancheri C, Sortino MA, Tomaselli V, et al (2000) Different expression of TNF-alpha receptors and prostaglandin E(2)Production in normal and fibrotic lung fibroblasts: potential implications for the evolution of the inflammatory process. Am J Respir Cell Mol Biol 22:628–634. https://doi.org/10.1165/ajrcmb.22.5.3948

Wang L, Scabilloni JF, Antonini JM, et al (2006) Induction of secondary apoptosis, inflammation, and lung fibrosis after intratracheal instillation of apoptotic cells in rats. Am J Physiol Lung Cell Mol Physiol 290:L695–L702. https://doi.org/10.1152/ajplung.00245.2005

Wang R, Alam G, Zagariya A, et al (2000) Apoptosis of lung epithelial cells in response to TNF-alpha requires angiotensin II generation de novo. J Cell Physiol 185:253–259. https://doi.org/10.1002/1097-4652(200011)185:2<253::AID-JCP10>3.0.CO;2-#

Wilborn J, Crofford LJ, Burdick MD, et al (1995) Cultured lung fibroblasts isolated from patients with idiopathic pulmonary fibrosis have a diminished capacity to synthesize prostaglandin E2 and to express cyclooxygenase-2. J Clin Invest 95:1861–1868. https://doi.org/10.1172/JCI117866

Figures

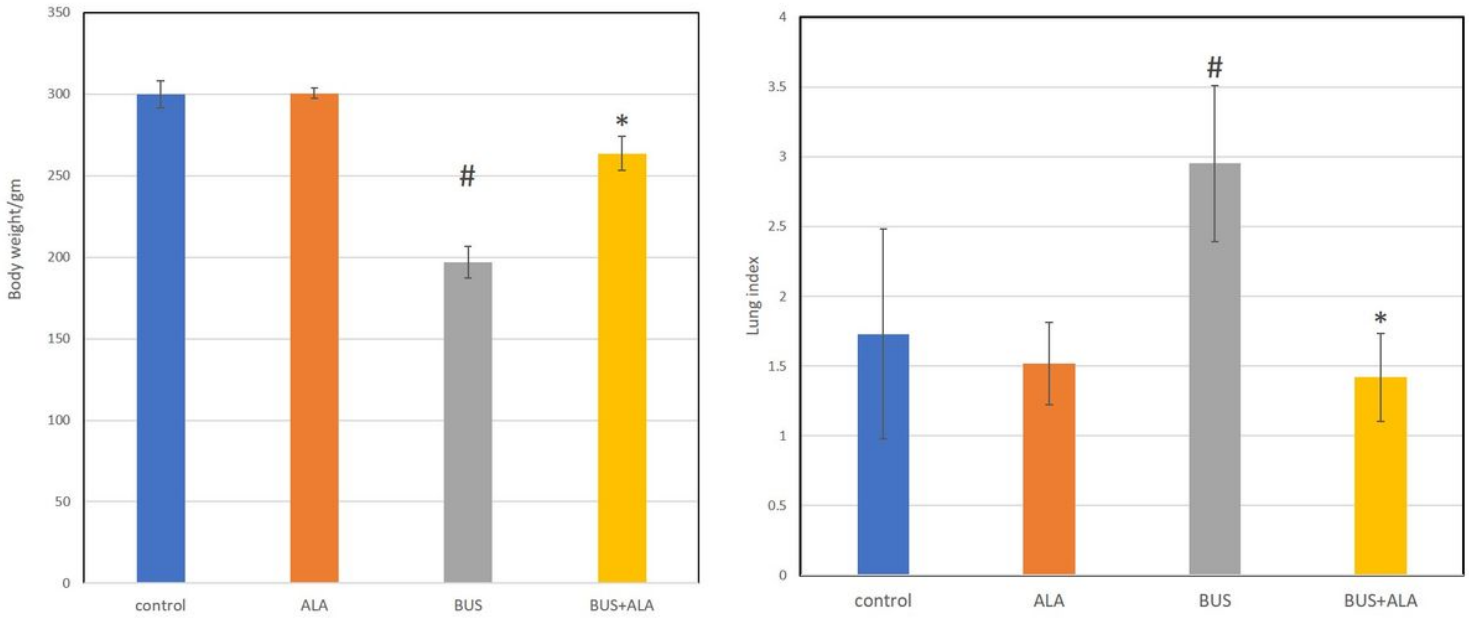

Figure 1

Effects of ALA on the final body weight and lung index in all experimental groups. The test used: One-way ANOVA followed by posthoc Tukey's test. Data are expressed as mean ± SD, # represents significance compared to the control group; * represents significance compared with the BUS group.

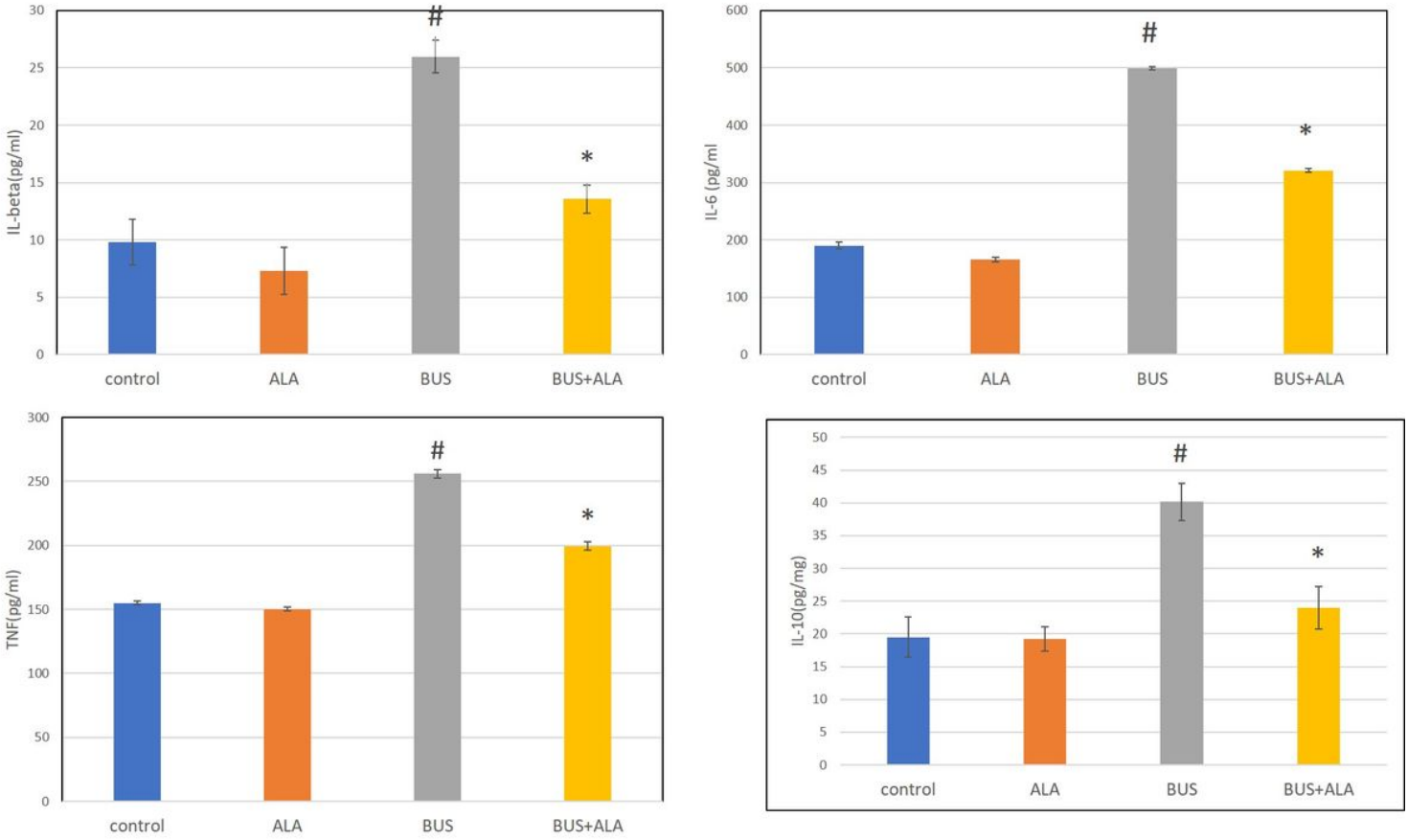

Figure 2

Effects of ALA on the serum levels of proinflammatory cytokines in all experimental groups. The test used: One-way ANOVA followed by posthoc Tukey's test. Data are expressed as mean ± SD, # represents significance compared to the control group; * represents significance compared with the BUS group.

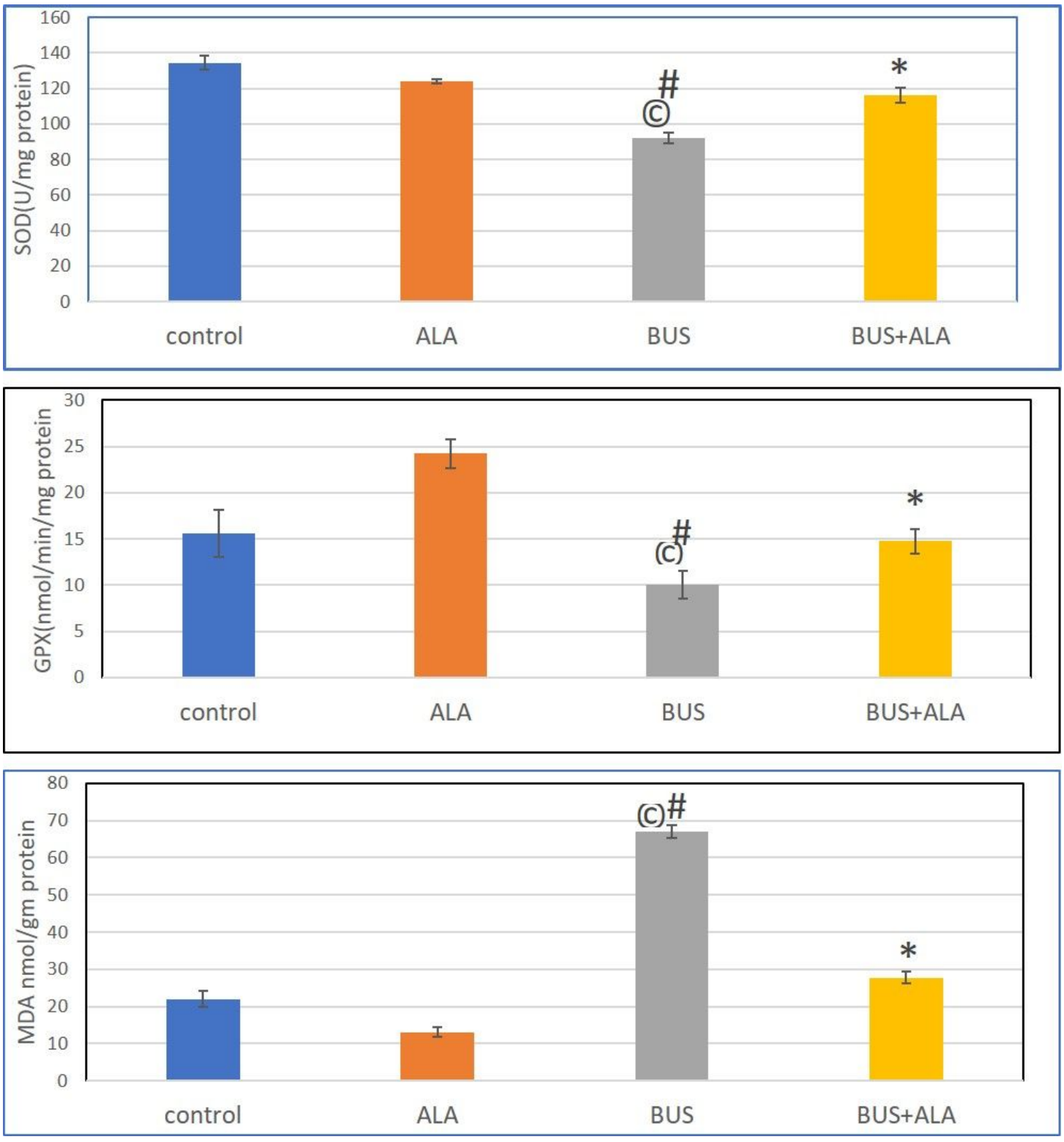

Figure 3

Effects of ALA on the oxidant state in the lung tissues of all experimental groups. The test used: One-way ANOVA followed by posthoc Tukey's test. Data are expressed as mean ± SD, # represents significance compared to the control group; * represents significance compared with the BUS group; © represents significance compared to the ALA group.

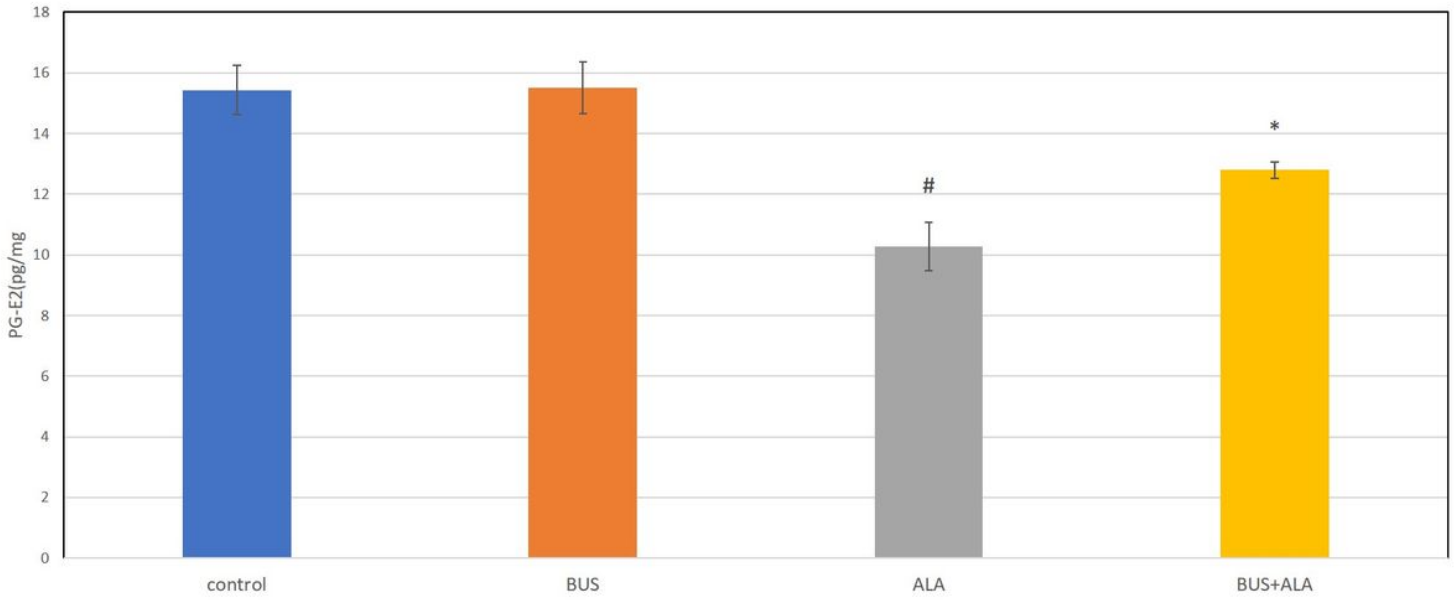

Figure 4

Effect of ALA on the level of PGE2 in the lung tissues of different groups. The test used: One-way ANOVA followed by posthoc Tukey's test. Data are expressed as mean ± SD, # represents significance compared to the control group; * represents significance compared with the BUS group.

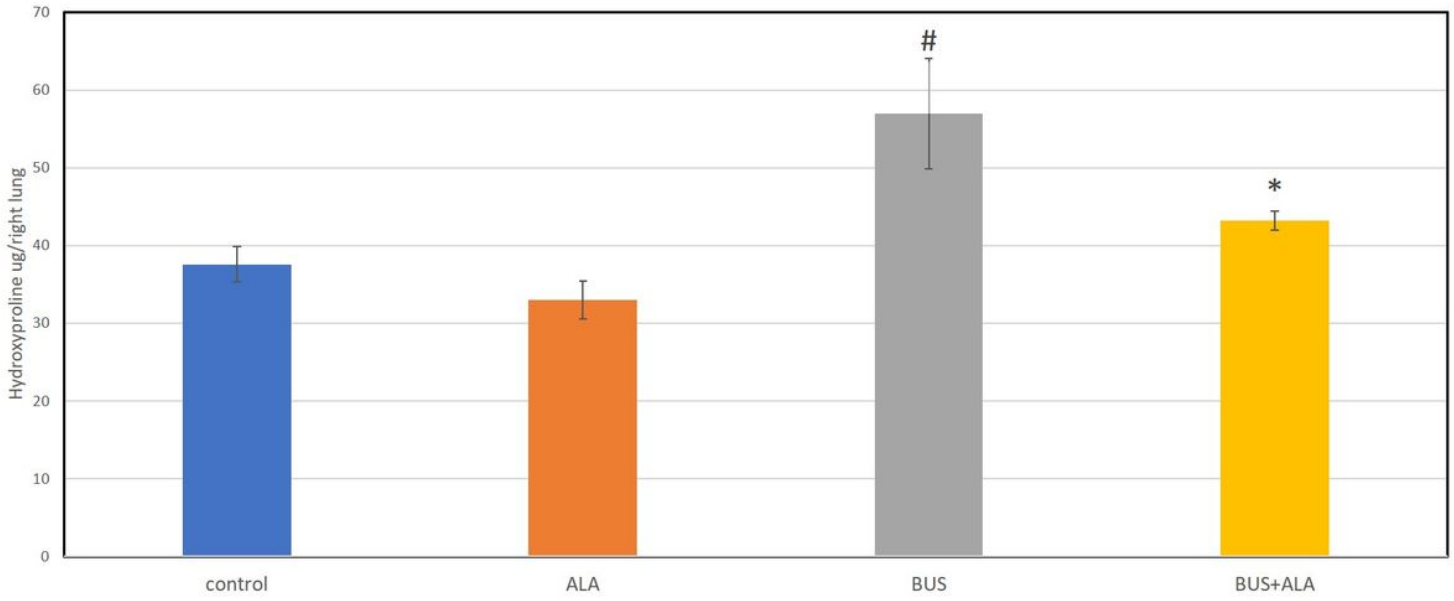

Figure 5

Effect of ALA on the hydroxyproline content in the lung tissues of all experimental groups. The test used: One-way ANOVA followed by posthoc Tukey's test. Data are expressed as mean ± SD, # represents significance compared with the control group; * represents significance compared with the BUS group.

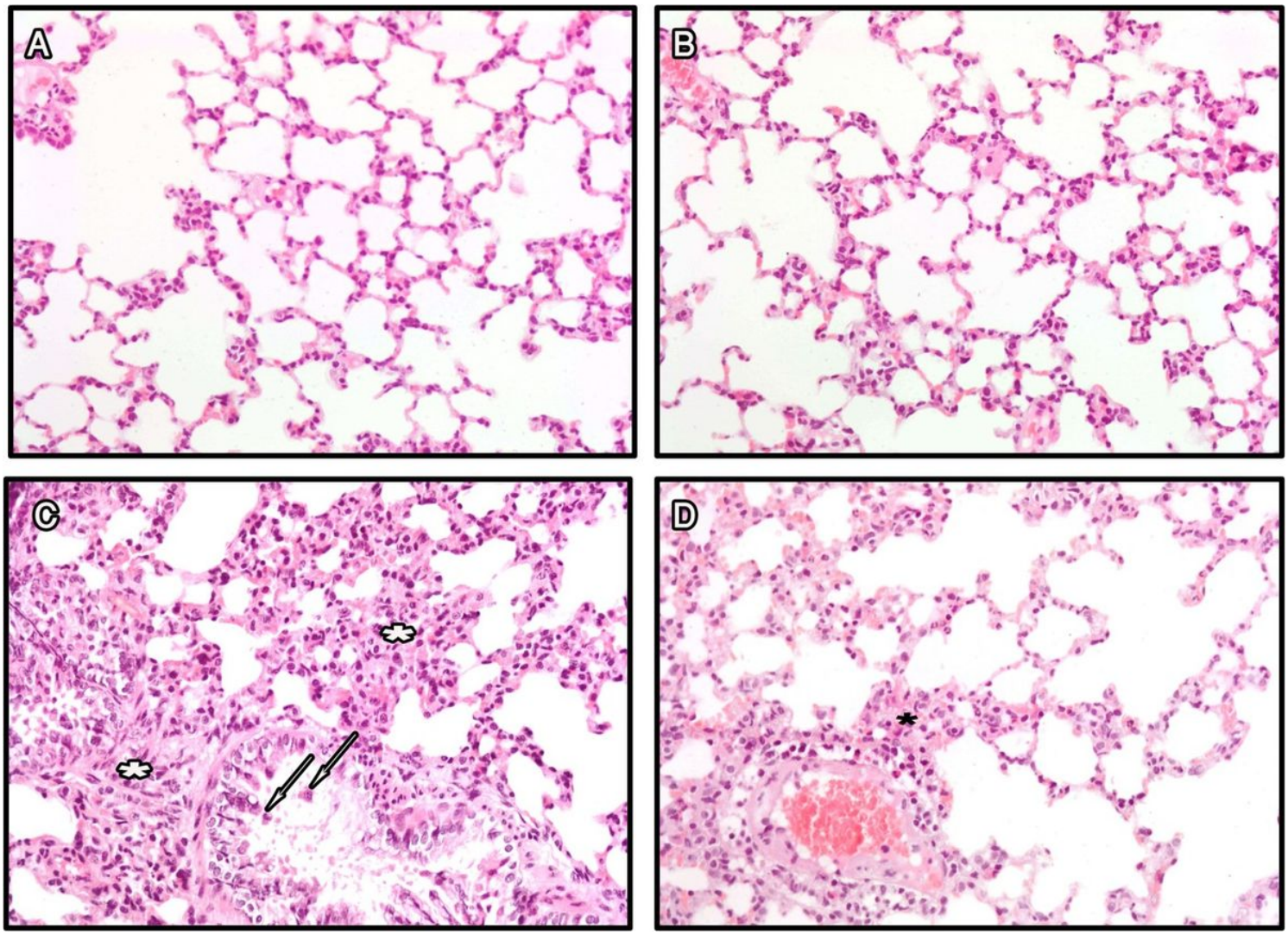

Figure 6

Photomicrographs of H and E stained lung sections of different groups. lung sections of the control group and ALA group (A & B respectively) show normal lung architecture. The lung section of BUS group (C) shows a disorganized architecture of the lung, increased cellular infiltration (white asterisks), and pulmonary bronchiole contains intraluminal cellular debris (arrows). The lung section of the BUS + ALA group (D) shows more or less organized lung architecture and mild cellular infiltration (black asterisk) (H&E stain x 400)

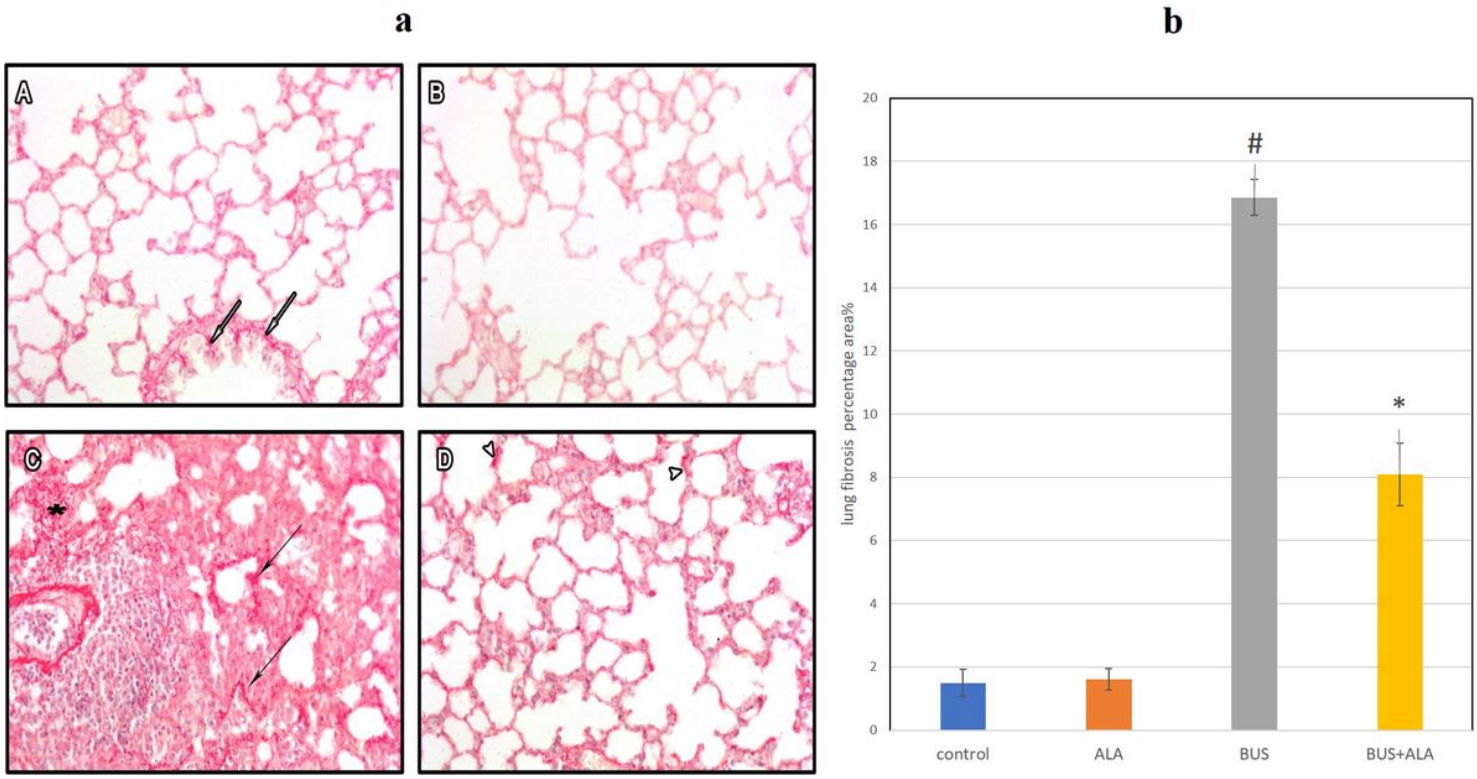

Figure 7

a) Photomicrographs of Sirus red-stained lung sections of different groups: lung sections of the control group and ALA group (A & B respectively) show normal collagen distribution in both pulmonary interstitium and the bronchiolar wall (white arrows). The lung section of BUS group (C) shows excessive collagen deposition in the pulmonary interstitium (black asterisk) and the surrounding alveolar wall (black arrows). The lung section of the BUS + ALA group (D) shows less marked interstitial collagen deposition (arrowheads) (Sirus red stain x 400). b) The percentage area of fibrosis in all experimental groups. The test used: One-way ANOVA followed by posthoc Tukey's test. Data are expressed as mean ± SD, # represents significance compared to the control group; * represents significance compared to the BUS group.

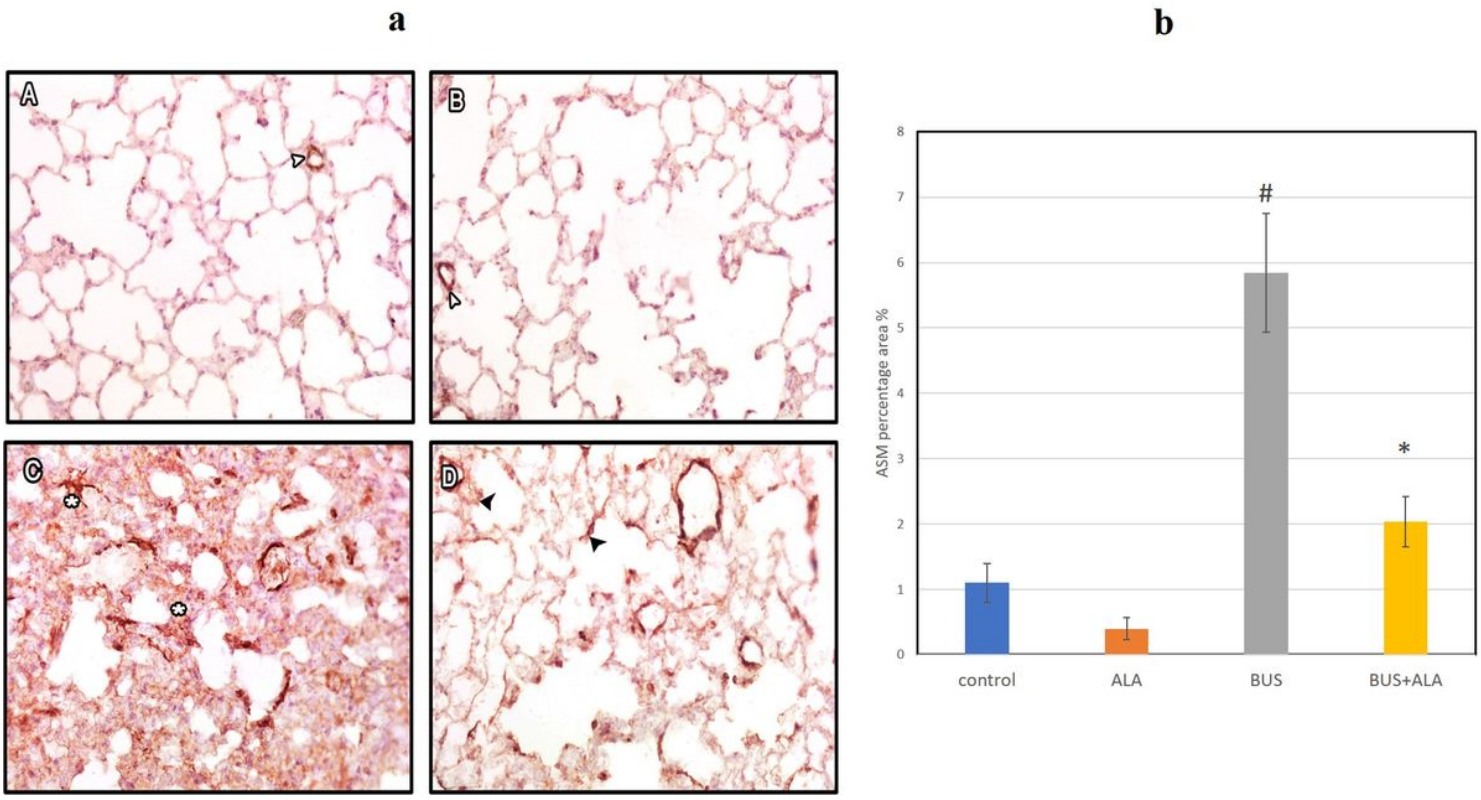

Figure 8

: a) Photomicrographs of α-smooth muscle actin (α-SMA) immuno-stained lung sections of different groups: lung sections of the control group and ALA group (A & B respectively) show normally immuno-positive reaction around blood vessels (white arrowheads). The lung section of BUS group (C) shows markedly increased immuno-positive reaction in the pulmonary interstitium (asterisk). The lung section of the BUS + ALA group (D) shows mild immuno-positive reaction (black arrowheads) (α-SMA immune stain x 400). b) The percentage area of α-SMA in all experimental groups. The test used: One-way ANOVA followed by posthoc Tukey's test. Data are expressed as mean ± SD, # represents significance compared with the control group; * represents significance compared with the BUS group.

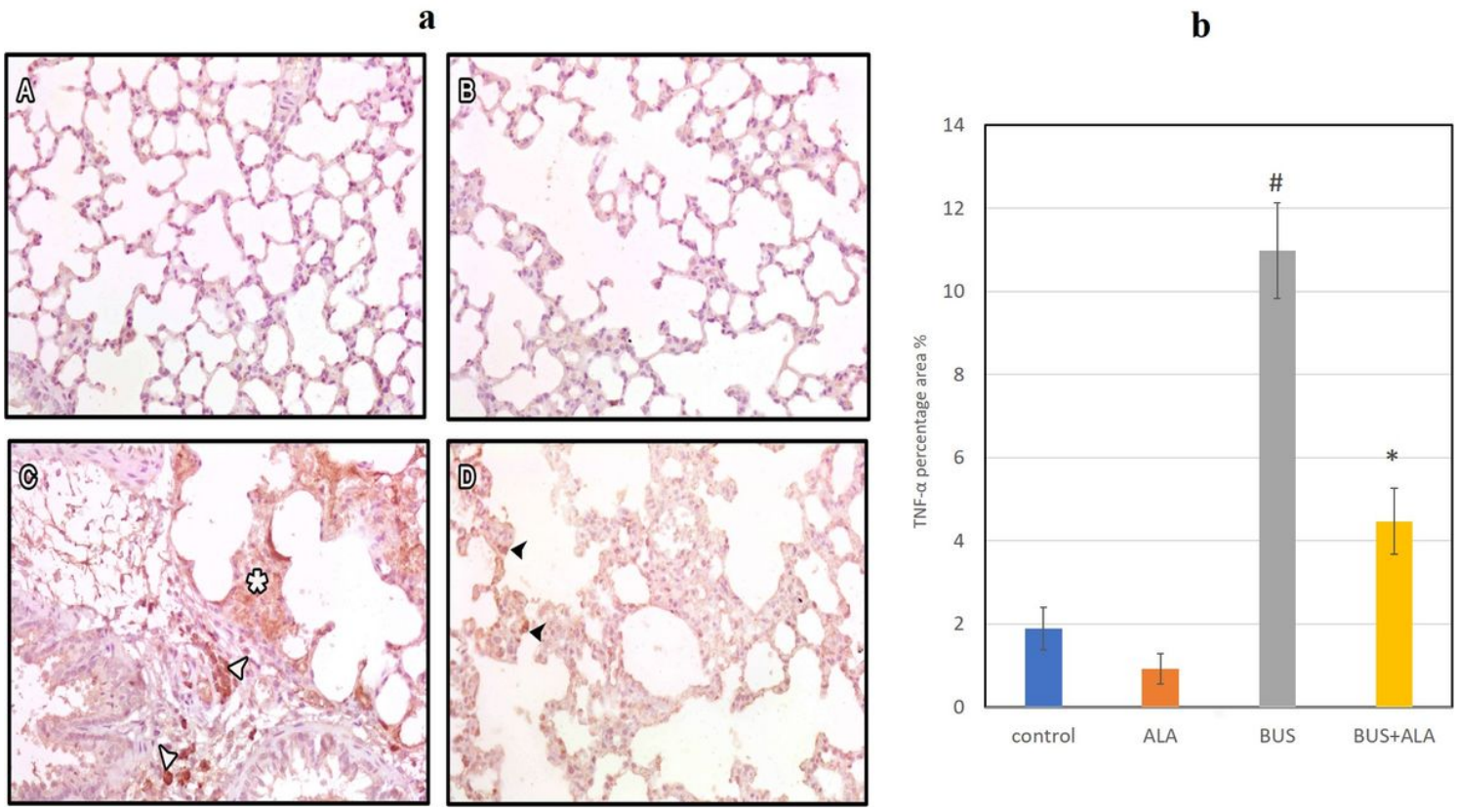

Figure 9

Photomicrographs of Tumor necrosis factor-α (TNF-α) immuno-stained lung sections of different groups: lung sections of the control group and ALA group (A & B respectively) show a negative immune reaction. The lung section of BUS group (C) shows markedly increased immuno-positive reaction in the pulmonary interstitium (asterisk) and mononuclear cells (white arrowheads). The lung section of BUS +ALA group IV (D) shows the mild immuno-positive reaction in the pulmonary interstitium (black arrowheads) (TNF-α immune stain x 400). b) The percentage area of TNF-α in all experimental groups. The test used: One-way ANOVA followed by posthoc Tukey's test. Data are expressed as mean ± SD, # represents significance compared with the control group; * represents significance compared with the BUS group.

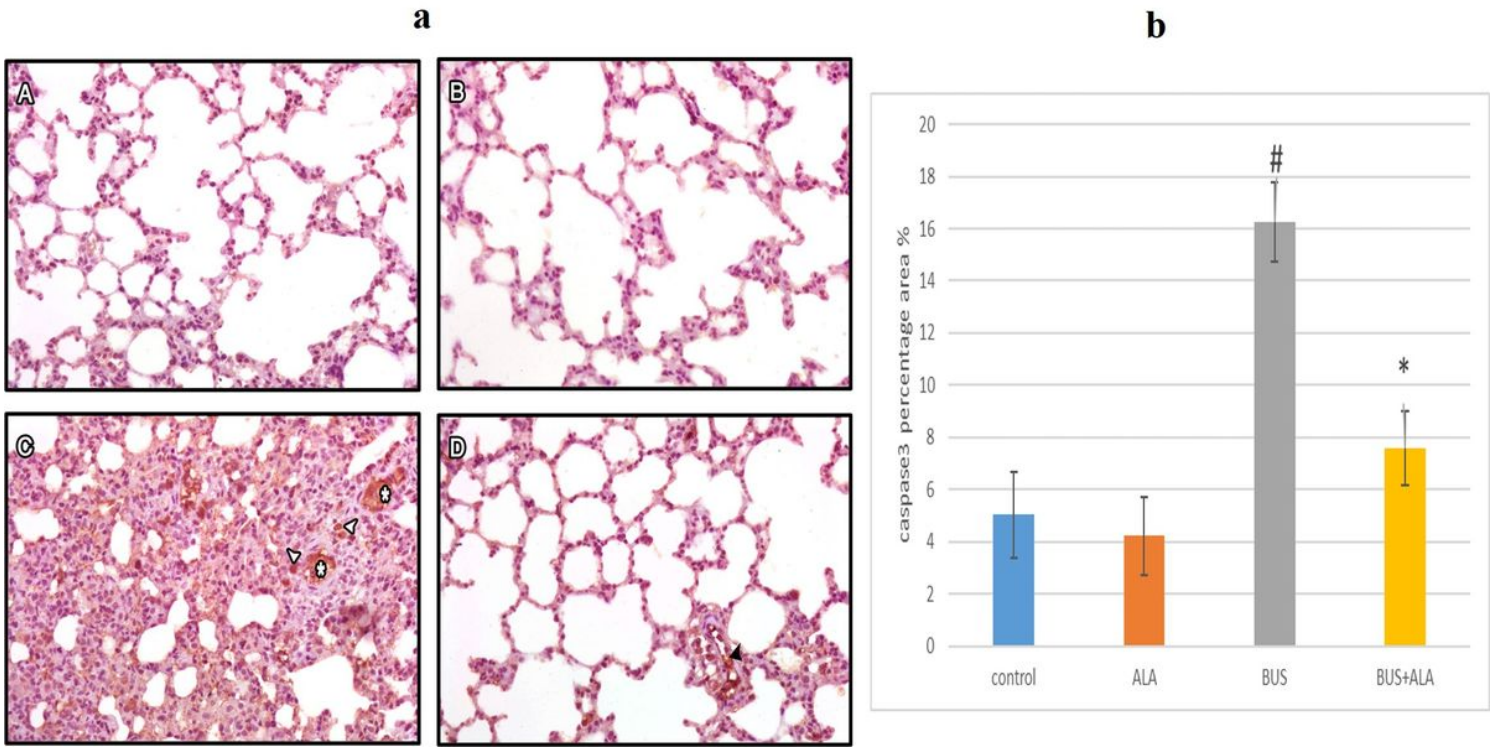

Figure 10

a) Photomicrographs of caspase 3 immuno-stained lung sections of different groups: lung sections of the control group and ALA group (A & B respectively) show a negative immune reaction. The lung section of BUS group (C) shows markedly increased immuno-positive reaction in the pulmonary interstitium (asterisks) and mononuclear cells (white arrowheads). The lung section of the BUS + ALA group (D) shows the mild immuno-positive reaction in mononuclear cells (black arrowhead) (caspase 3 immune stain x 400). b) The percentage area of caspase 3 in all experimental groups. The test used: One-way ANOVA followed by posthoc Tukey's test. Data are expressed as mean ± SD, # represents significance compared with the control group; * represents significance compared with the BUS group; © represents significance compared with the ALA group.

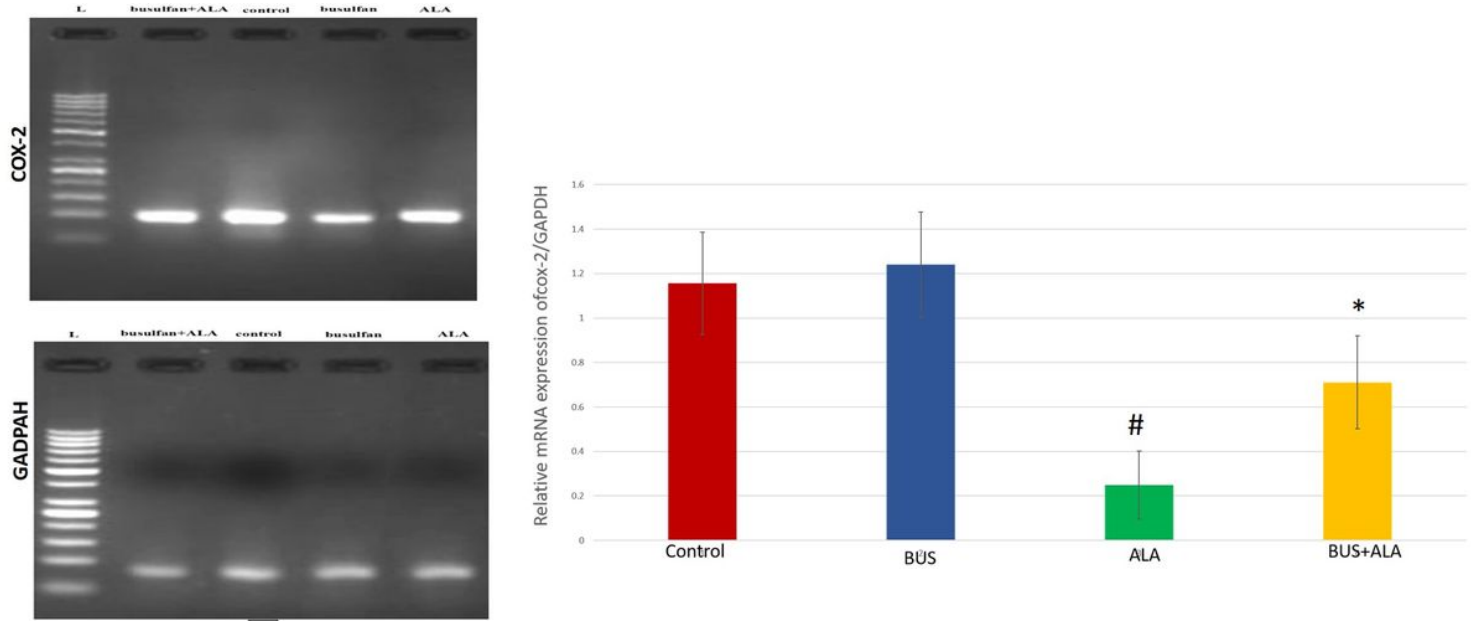

Figure 11

Effect of ALA on the pulmonary mRNA expression of COX-2 in different groups. The test used: One-way ANOVA followed by posthoc Tukey's test. Data are expressed as mean ± SD, * represents significance compared with the control group; # represents significance compared with the BUS group

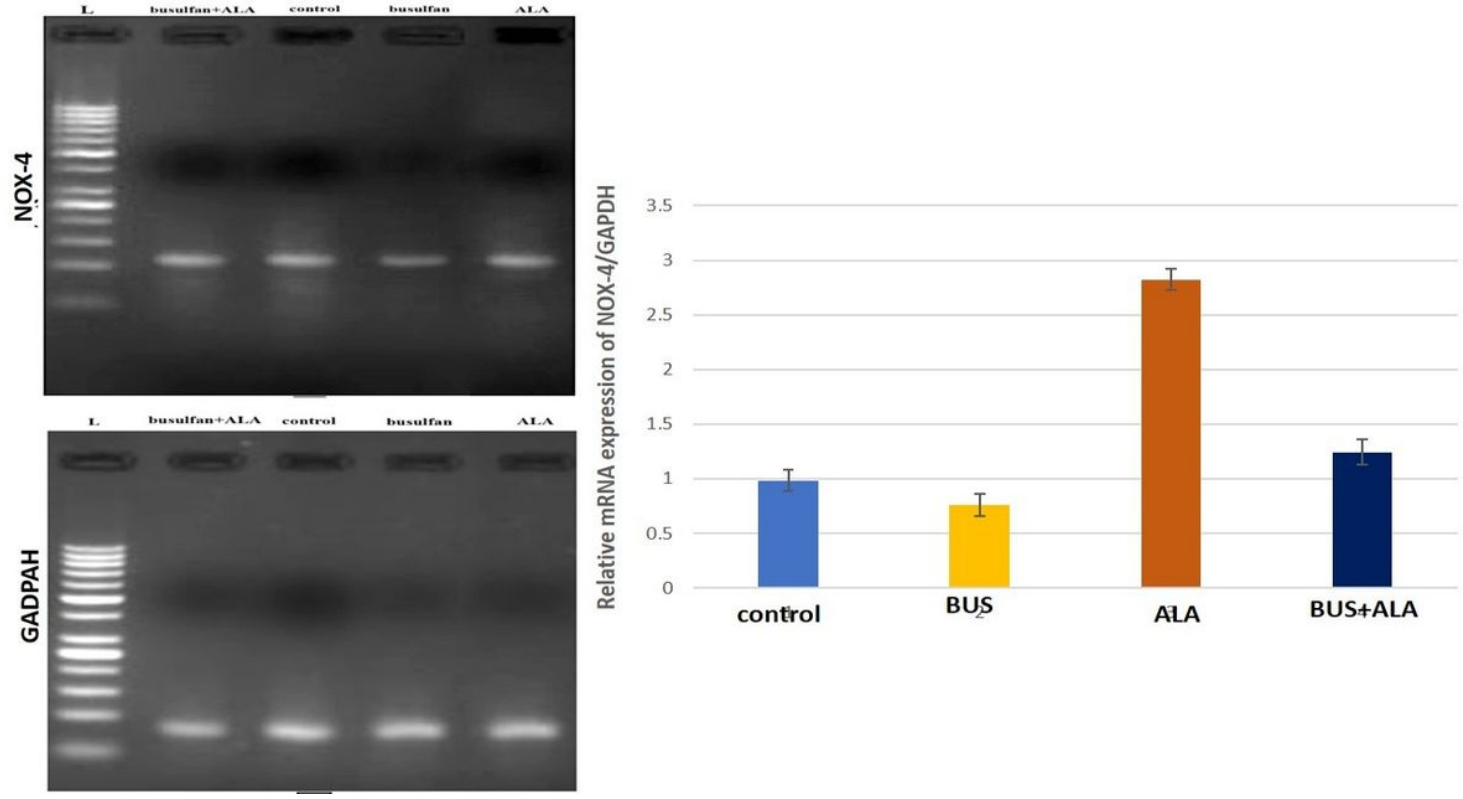

Figure 12

Effect of ALA on the pulmonary mRNA expression of NOX-4 all experimental groups. The test used: One-way ANOVA followed by posthoc Tukey's test. Data are expressed as mean ± SD, * represents significance

compared with the control group; # represents significance compared with the BUS group

Supplementary Files

This is a list of supplementary files associated with this preprint. Click to download.

- rawdata.xlsx